PROCEEDINGS OF SCIENCE

Updates on the parity-odd structure function of the nucleon from the Compton amplitude

K. U. Can,[a,*] J. A. Crawford,[a] R. Horsley,[b] P. E. L. Rakow,[d] T. G. Schar,[a] G. Schierholz,[e] H. Stüben,[f] R. D. Young[a] and J. M. Zanotti[a]

[a] *CSSM, Department of Physics, The University of Adelaide, Adelaide SA 5005, Australia.*
[b] *School of Physics and Astronomy, University of Edinburgh, Edinburgh EH9 3JZ, UK.*
[c] *RIKEN Center for Computational Science, Kobe, Hyogo 650-0047, Japan.*
[d] *Theoretical Physics Division, Department of Mathematical Sciences, University of Liverpool, Liverpool L69 3BX, United Kingdom.*
[e] *Deutsches Elektronen-Synchrotron DESY, Notkestr. 85, 22607 Hamburg, Germany.*
[f] *Regionales Rechenzentrum, Universität Hamburg, 20146 Hamburg, Germany.*

E-mail: kadirutku.can@adelaide.edu.au

The parity-odd structure function, F_3, accessible via neutrino-nucleon deep-inelastic scattering, plays an important role in estimating the hadronic uncertainties in the extracted weak parameters of the Standard Model (SM). Controlled and reduced uncertainties in SM processes are crucial for beyond the standard model searches progressing via CKM matrix elements or the weak mixing angle. The electroweak box diagrams contribute the dominant theoretical uncertainty and can be related to the lowest Nachtmann moment of F_3 through a dispersive approach, enabling a model-independent estimation of their contributions. Unfortunately, the experimental data for F_3 either do not exist or belong to a separate isospin channel which requires modelling, thus making it challenging to control the systematic uncertainties. Therefore a first-principles calculation of F_3 is highly desirable to reliably calculate the electroweak boxes. Additionally, the Gross-Llewellyn Smith (GLS) sum rule is also associated with the lowest moment of F_3 structure function and in the parton model, it counts the number of valence quarks in a nucleon, with known perturbative corrections up to $O(\alpha_s^4)$. A precise first-principles determination of the Q^2 dependence of the GLS sum rule would therefore provide a pathway to an extraction of α_s from an hadronic observable.

We provide an update on the QCDSF Collaboration's progress in calculating the lowest moment of the F_3 structure function from the forward Compton amplitude at the SU(3) symmetric point. We study the Q^2 dependence of the lowest moment and give a comparison to the GLS sum rule. We discuss the effects of higher-twist/power corrections, extraction of α_s, and a possible determination of electroweak box contributions.

The 41st International Symposium on Lattice Field Theory (LATTICE2024)
28 July - 3 August 2024
Liverpool, UK

*Speaker

https://pos.sissa.it/

PoS(LATTICE2024)326

1. Introduction

Deep-inelastic neutrino-nucleon scattering contains important information on radiative corrections of weak decays and parity violating lepton-nucleon interactions encoded through the exchange of a photon and a heavy W/Z gauge boson, i.e. the electroweak box diagram. One of the major sources of theoretical uncertainty in the determination of the CKM matrix elements and the weak mixing angle at low scales [1, 2] are the radiative corrections. Additionally, experimental programs probing the neutrino oscillation such as [3], would benefit from precise parity-odd structure functions, particularly for large Bjorken-x and at the highest energies of the DUNE [4] beam. Furthermore, weak currents, unlike the electromagnetic current, couple nontrivially to spin and flavour [5, 6], thus providing useful constraints on the spin and flavour decomposition of parton distribution functions (PDFs) [6].

Lattice QCD is well-positioned to provide first-principles determinations of the structure functions. The QCDSF collaboration has been pursuing the calculations of the moments of structure functions from the Compton amplitude calculated by a Feynman-Hellmann approach initiated in [7] and applied to unpolarised [8, 9] and polarised [10] parity-conserving nucleon structure functions. In this contribution, we provide an update on our previous report [11] which gave an account of our calculations on the unpolarised parity-odd structure function. The calculation of the Q^2 dependence of the lowest moment of $F_3^{\gamma Z}$ using a Feynman-Hellmann approach is the focus of this contribution. The lowest moment of the parity-odd structure function is of particular importance since it can be related to the electroweak box diagram contribution via a dispersion relation,

$$\Box_{VA}^{\gamma W} = \frac{3\alpha_{EM}}{2\pi} \int_0^\infty \frac{dQ^2}{Q^2} \frac{M_W^2}{M_W^2 + Q^2} \mu_1^{(3)}(Q^2), \tag{1}$$

where α_{EM} is the fine-structure constant, M_W is the mass of the W boson, and $\mu_1^{(3)}$ is the first Nachtmann moment of the flavour non-diagonal structure function $F_3^{\gamma W}$. In [12] Ma et al. have presented a recent lattice QCD calculation of the γW-box contribution to superallowed nuclear and neutron beta decays. A dispersion relation analogous to Eq. (1) can be written for the γZ box diagram. Isospin symmetry provides the relation, $F_3^{\gamma W} \equiv (F_3^{\gamma Z,p} - F_3^{\gamma Z,n})/4$, between the flavour non-diagonal and flavour diagonal structure functions.

In addition to its connection to the γW-box contribution, the first moment of γZ interference structure function provides a significant test of the Gross–Llewellyn Smith (GLS) sum rule. In the quark-parton model the first moment of $F_3^{\gamma Z}$ is proportional to the number of valence quarks in the nucleon, it is a non-singlet quantity, and it has a vanishing anomalous dimension at leading order in QCD [13], making the GLS sum rule a very clean quantity to study. The QCD corrections for the leading twist contribution of the GLS sum rule has been computed to N^{3}LO [13–15] and the power corrections have been addressed in model calculations [16–18], although with widely varying results. A first-principles calculation would therefore provide insights to the interplay between the perturbative and nonperturbative regimes.

The rest of this contribution is organised as follows: In Sec. 2 we discuss the decomposition of the Compton amplitude and the kinematics to isolate the parity-odd Compton structure function $\mathcal{F}_3$. A brief summary of the Feynman-Hellmann approach employed to calculate the Compton amplitude is given in Sec. 3, followed by the preliminary results in Sec. 4. Our concluding remarks are given in Sec. 5.

2. Parity-odd Compton amplitude

The starting point of the calculation is the time-ordered product of vector and axial vector currents, J_μ and J^A_ν, sandwiched between nucleon states, forming the hadronic tensor,

$$T_{\mu\nu}(p,q) = i\rho_{ss'} \int d^4 z e^{iq\cdot z} \langle p, s' | \mathcal{T}\{J_\mu(z) J^A_\nu(0)\} | p, s\rangle, \tag{2}$$

where p (q) is the nucleon (current) momentum, and $\rho_{ss'}$ is the spin density matrix. The Lorentz decomposition of the hadronic tensor for the spin-averaged case involves six structure functions [19, 20],

$$\begin{aligned} T_{\mu\nu}(p,q) = &- g_{\mu\nu}\mathcal{F}_1(\omega,Q^2) + \frac{p_\mu p_\nu}{p\cdot q}\mathcal{F}_2(\omega,Q^2) + i\,\varepsilon_{\mu\nu}{}^{\alpha\beta}\frac{p_\alpha q_\beta}{2p\cdot q}\mathcal{F}_3(\omega,Q^2) \\ &+ \frac{q_\mu q_\nu}{p\cdot q}\mathcal{F}_4(\omega,Q^2) + \frac{p_{\{\mu}q_{\nu\}}}{p\cdot q}\mathcal{F}_5(\omega,Q^2) + \frac{p_{[\mu}q_{\nu]}}{p\cdot q}\mathcal{F}_6(\omega,Q^2), \end{aligned} \tag{3}$$

where $\varepsilon^{0123} = 1$, $\omega = 2p\cdot q/Q^2$, and $p_{\{\mu}q_{\nu\}} = (p_\mu q_\nu + p_\nu q_\mu)/2$ and $p_{[\mu}q_{\nu]} = (p_\mu q_\nu - p_\nu q_\mu)/2$ denote the symmetrisation and antisymmetrisation of the indices respectively. Here, $\mathcal{F}_{1,2}$ are the familiar unpolarised Compton structure functions. Since the axial charge is not conserved and the parity is violated, there are additional structure functions. $\mathcal{F}_{4,5}$ are not related to $\mathcal{F}_{1,2}$ by gauge invariance any more so they survive, and $\mathcal{F}_{3,6}$ are allowed because the parity is violated, although $\mathcal{F}_6 = 0$ due to the time reversal invariance of strong interactions.

We are interested in the $\mathcal{F}_3$ amplitude, which is the only surviving parity-violating part. Choosing the off-diagonal components of the tensor, e.g. $\mu \neq \nu$, and $p_\mu = q_\mu = 0$, it is straightforward to isolate $\mathcal{F}_3$,

$$T_{\mu\nu}(p,q) = i\,\varepsilon_{\mu\nu}{}^{\alpha\beta}\frac{p_\alpha q_\beta}{2p\cdot q}\mathcal{F}_3(\omega,Q^2), \tag{4}$$

which is connected to the unpolarised parity-violating structure function F_3 through the dispersion relation,

$$\mathcal{F}_3(\omega,Q^2) = 4\omega \int_0^1 dx \frac{F_3(x,Q^2)}{1-x^2\omega^2}. \tag{5}$$

Upon expanding the geometric series we arrive at,

$$\frac{\mathcal{F}_3(\omega,Q^2)}{\omega} = 4 \sum_{n=1,2,\dots} \omega^{2n-2} M^{(3)}_{2n-1}(Q^2), \tag{6}$$

with the odd Mellin moments of F_3 defined as,

$$M^{(3)}_{2n-1}(Q^2) = \int_0^1 dx\, x^{2n-2} F_3(x,Q^2), \quad \text{for } n = 1,2,3,\dots \tag{7}$$

We note that the lowest Mellin moment, $M^{(3)}_1(Q^2)$, is directly accessible at $\omega = 0$, i.e. for a nucleon at rest, thus can be extracted from the Compton amplitude without a polynomial fit in ω.

3. Feynman-Hellmann approach

Now the task is to calculate the Compton amplitude. An analysis of the Compton amplitude requires the evaluation of lattice four-point correlation functions. However, this is not an easy task given the rapid deterioration of the signal for large time separations and the contamination due to excited states. The application of the Feynman-Hellmann theorem reduces the problem to a simpler analysis of two-point correlation functions using the established techniques of spectroscopy. Our implementation of the second order Feynman-Hellmann method is presented in detail in [8].

To compute the hadronic tensor, Eq. (2), that involves the product of a vector and axial vector currents, the Feynman-Hellmann technique needs to be generalised to mixed currents which has been done in the context of generalised parton distribution calculations before [21], albeit for electromagnetic currents. It is also clear from Eq. (4) that we need the antisymmetric part of the tensor. In this case, we introduce two spatially oscillating background fields to the action

$$S(\boldsymbol{\lambda}) = S_0 + \lambda_1 \int d^4z \cos(q \cdot z) \mathcal{J}_\mu(z) + \lambda_2 \int d^4y \sin(q \cdot y) \mathcal{J}_\nu^A(y), \tag{8}$$

where S_0 is the unperturbed action, λ_1, λ_2 are the strengths of the couplings between the quarks and the external fields, and $\boldsymbol{\lambda} \equiv (\lambda_1, \lambda_2)$; $\mathcal{J}_\mu(z) = Z_V \bar{q}(z)\gamma_\mu q(z)$ and $\mathcal{J}_\nu^A(y) = Z_A \bar{q}(y)\gamma_5\gamma_\nu q(y)$ are the renormalised vector and axial vector currents coupling to the quarks along the μ and ν directions, $q = (0, \mathbf{q})$ is the external momentum inserted by the currents and $Z_{V,A}$ are the renormalisation constants for the local vector and axial vector currents. We note that a multiplicative renormalisation is the only renormalisation that is needed in the Feynman-Hellmann approach where $Z_{V,A}$ are determined before [22]. Following the derivation presented in [8], we arrive at the Feynman-Hellmann relation between the second-order energy shift and the Compton amplitude,

$$\left.\frac{\partial^2 E_{N_\lambda}(\mathbf{p}, \mathbf{q})}{\partial \lambda_1 \partial \lambda_2}\right|_{\lambda=0} = i\frac{T_{\mu\nu}(p, q) - T_{\mu\nu}(p, -q)}{2E_N(\mathbf{p})} \tag{9}$$

where $T_{\mu\nu}$ is the Compton amplitude defined in Eq. (2), and $E_{N_\lambda}(\mathbf{p}, \mathbf{q})$ is the nucleon energy at momentum $\mathbf{p}$ in the presence of a background field of strength $\boldsymbol{\lambda}$. For an independent derivation, based on an expansion of the Lagrangian in terms of a periodic external source [23], see [24].

4. Preliminary results

The parity-odd Compton structure function $\mathcal{F}_3$, is isolated through a choose of kinematics $\mu = 1$, $\nu = 3$, $\alpha = 0$, $\beta = 2$, $\mathbf{p}_1 = \mathbf{q}_1 = 0$ and $\mathbf{q}_2 \neq 0$. Noting that $q_0 = 0$ in the FH approach, we rewrite Eq. (4) as

$$\frac{\mathcal{F}_3(\omega, Q^2)}{\omega} = \frac{Q^2}{\mathbf{q}_2} \left.\frac{\partial^2 E_{N_\lambda}(\mathbf{p})}{\partial \lambda_1 \partial \lambda_2}\right|_{\lambda=0}, \tag{10}$$

Here we remind the reader that in practice, we determine the RHS of Eq. (10) which is well defined.

The following ratio allows us to extract the energy shift,

$$\mathcal{R}_\lambda(\mathbf{p}, \mathbf{q}, t) \equiv \frac{G^{(2)}_{+\lambda_1,+\lambda_2}(\mathbf{p}, \mathbf{q}, t)\, G^{(2)}_{-\lambda_1,-\lambda_2}(\mathbf{p}, \mathbf{q}, t)}{G^{(2)}_{+\lambda_1,-\lambda_2}(\mathbf{p}, \mathbf{q}, t)\, G^{(2)}_{-\lambda_1,+\lambda_2}(\mathbf{p}, \mathbf{q}, t)} \xrightarrow{t \gg 0} A_\lambda(\mathbf{p}) e^{-4\Delta E^{oo}_{N_\lambda}(\mathbf{p}, \mathbf{q})\, t}, \tag{11}$$

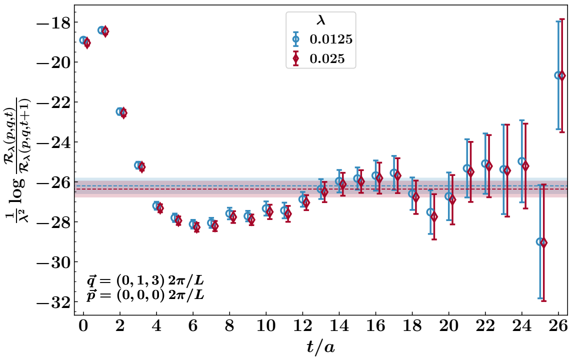

Figure 1: Effective mass plot of the ratio (Eq. (11)). The energy shifts determined via a weighted averaging procedure are shown by the shaded bands. We are showing the results for the uu contribution, for $(\mathbf{p}, \mathbf{q}) = ((0,0,0),(0,1,3))\left(\frac{2\pi}{L}\right)$ corresponding to $\omega = 0.0$ at $Q^2 \sim 2.5\,\text{GeV}^2$.

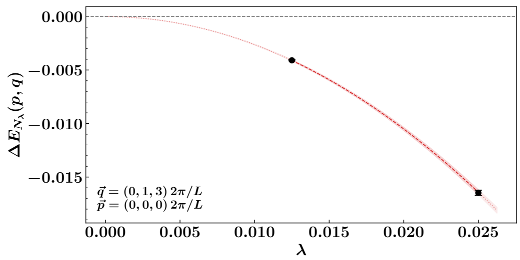

Figure 2: λ dependence of the extracted energy shift for the same kinematics given in Fig. 1. The uncertainty of the $\lambda = 0.0125$ point is smaller than the symbol.

where $\Delta E^{oo}_{N_\lambda}(\mathbf{p},\mathbf{q})$ is the energy shift, and $A_\lambda(\mathbf{p})$ is the overlap factor which is irrelevant for our discussion of energy shifts. The ratio (Eq. (11)) isolates the energy shift only at even orders of $\boldsymbol{\lambda}$, e.g. $O(\lambda_1^n\lambda_2^m)$ with $n+m$ even and $n, m \geq 0$. Here, $G^{(2)}_{\lambda_1,\lambda_2}(\mathbf{p},\mathbf{q},t) \xrightarrow{t\gg 0} A'_\lambda(\mathbf{p})e^{-E_{N_\lambda}(\mathbf{p},\mathbf{q})t}$, is the perturbed two-point function with $\lambda_1 = \lambda_2 = \lambda$, where $A_\lambda(\mathbf{p})$ is the overlap factor and $E_{N_\lambda}(\mathbf{p},\mathbf{q})$ is the perturbed energy of the ground state. The relation between $\Delta E^{oo}_{N_\lambda}(\mathbf{p},\mathbf{q})$ and the Compton amplitude is rendered visible when considering the perturbed energy of the nucleon expanded as a Taylor series in the limit $\boldsymbol{\lambda} \to 0$,

$$E_{N_\lambda}(\mathbf{p},\mathbf{q}) = E_N(\mathbf{p}) + \Delta E^{eo}_{N_\lambda}(\mathbf{p},\mathbf{q}) + \Delta E^{oe}_{N_\lambda}(\mathbf{p},\mathbf{q}) + \Delta E^{ee}_{N_\lambda}(\mathbf{p},\mathbf{q}) + \Delta E^{oo}_{N_\lambda}(\mathbf{p},\mathbf{q}), \tag{12}$$

where the superscript e (o) denote the terms even (odd) in $\lambda_{1,2}$. The term of interest is,

$$\Delta E^{oo}_{N_\lambda}(\mathbf{p},\mathbf{q}) = \lambda_1\lambda_2 \left.\frac{\partial^2 E_{N_\lambda}(\mathbf{p},\mathbf{q})}{\partial\lambda_1\partial\lambda_2}\right|_{\lambda=0} + O(\lambda_1\lambda_2^3) + O(\lambda_1^3\lambda_2), \tag{13}$$

which gives the energy shift associated with the interference of the currents $\mathcal{J}_\mu$ and $\mathcal{J}^A_\nu$ appearing on the LHS of Eq. (9).

Our calculations are performed on QCDSF's 2+1-flavour gauge configurations. Two ensembles are used with $V = 48^3 \times 96$, and couplings $\beta = 5.65$ and $\beta = 5.95$ corresponding to lattice spacings $a = 0.068$ fm and $a = 0.052$ fm, respectively. Quark masses are tuned to the $SU(3)$ symmetric point where the masses of all three quark flavours are set to approximately the physical flavour-singlet mass, $\overline{m} = (2m_s + m_l)/3$ [25, 26], yielding $m_\pi \approx 420$ MeV. We calculate the Compton structure function for photon momenta in the range, $0.5 \lesssim Q^2 \lesssim 10\ \text{GeV}^2$. Up to $O(10^3)$ measurements are performed to increase the statistics, equivalent to two sources on ensembles of size $O(500)$ configurations. Since F_3 is a non-singlet quantity we only calculate the connected diagrams.

All energy shifts, $\Delta E^{oo}_{N_\lambda}(\mathbf{p},\mathbf{q})$, are extracted by a single exponential fit to the ratio given in Eq. (11) for several fit windows to control the systematic uncertainty due to the choice of fit window via a weighted-averaging procedure outlined in [27]. We show a representative effective mass plot for the ratio for a nucleon at rest, $\mathbf{p} = (0,0,0)\left(\frac{2\pi}{L}\right)$, at $\mathbf{q} = (0,1,3)\left(\frac{2\pi}{L}\right)$ in Fig. 1.

To map the λ dependence of the energy shifts we calculate the ratio for $|\lambda| = [0.0125, 0.025]$ for each combination of $\mathbf{p}$ and $\mathbf{q}$ for each fit window. Then, we perform a polynomial fit using Eq. (13) to determine $\left.\frac{\partial^2 E_{N_\lambda}(\mathbf{p})}{\partial\lambda_1\partial\lambda_2}\right|_{\lambda=0}$. We do not find a statistically significant contamination due to neglected higher-order terms in Eq. (13). Our resulting fit is shown in Fig. 2. We have shown the weighted-average results in Figures 1 and 2 to demonstrate the intermediate steps, but in practice we perform the analysis for each time window until estimating the Compton amplitude (Eq. (10)). Our resulting $\mathcal{F}_3(\omega, Q^2)$ is shown in Fig. 3 for $\mathbf{p} = (0,0,0)\left(\frac{2\pi}{L}\right)$, at $\mathbf{q} = (0,1,3)\left(\frac{2\pi}{L}\right)$. In estimating the weighted-average value and the total uncertainty we use,

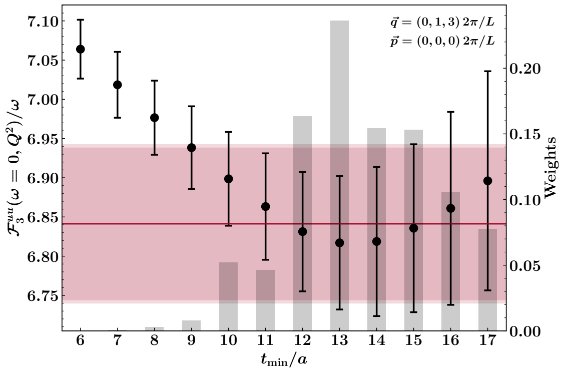

Figure 3: The $\mathcal{F}_3$ structure function for the same kinematics given in Fig. 1. We are showing the *uu* contribution calculated on the $\beta = 5.95$ ensemble. Grey bars associated with the y-axis indicate the weight of each point. The solid line is the weighted average and the inner and our shaded bands show the statistical and total uncertainties respectively.

$$\bar{O} = \sum_f w^f O^f, \qquad \delta_{\text{stat}}\bar{O}^2 = \sum_f w^f (\delta\bar{O}^f)^2, \tag{14}$$

$$\delta_{\text{sys}}\bar{O}^2 = \sum_f w^f (O^f - \bar{O})^2, \qquad \delta\bar{O} = \sqrt{\delta_{\text{stat}}\bar{O}^2 + \delta_{\text{sys}}\bar{O}^2}, \tag{15}$$

where O^f is an unbiased estimator the quantity of interest, e.g. $\mathcal{F}_3$, determined from the fit window f, δO^f is the statistical uncertainty of O^f estimated by a bootstrap analysis, and $\delta_{\text{stat}}\bar{O}$ and $\delta_{\text{sys}}\bar{O}$ are statistical and systematic uncertainties. The weight is given by $w^f = \frac{p_f\,(\delta O^f)^{-2}}{\sum_{f'} p_{f'}(\delta O^{f'})^{-2}}$, with $p_f = \Gamma(N_{\text{dof}}/2, \chi_f^2/2)/\Gamma(N_{\text{dof}}/2)$ the one-sided p-value.

The relation in Eq. (10) is derived starting from a continuum expression and has discretisation errors in a lattice formulation. We derive a correction factor for the kinematic term appearing in Eq. (10) through a lattice perturbation theory inspired procedure [28, 29] in order to reduce the effect of discretisation errors. The improvement is achieved by replacing the kinematic factor,

$$\frac{Q^2}{q_2} \to \frac{\sum_i \sin^2 q_i + [\sum_i (1 - \cos q_i)]^2}{\sin q_2}. \tag{16}$$

This correction reduces the discrepancy between the results obtained with different $\mathbf{q}$ momenta that correspond to the same Q^2 shown in Ref. [11]. We show our main result, the lowest odd moment of $F_3^{\gamma Z}$, for the isovector $uu - dd$ combination, $M^{(3)}_{1,uu-dd}(Q^2)$, in Fig. 4. We compare our moments

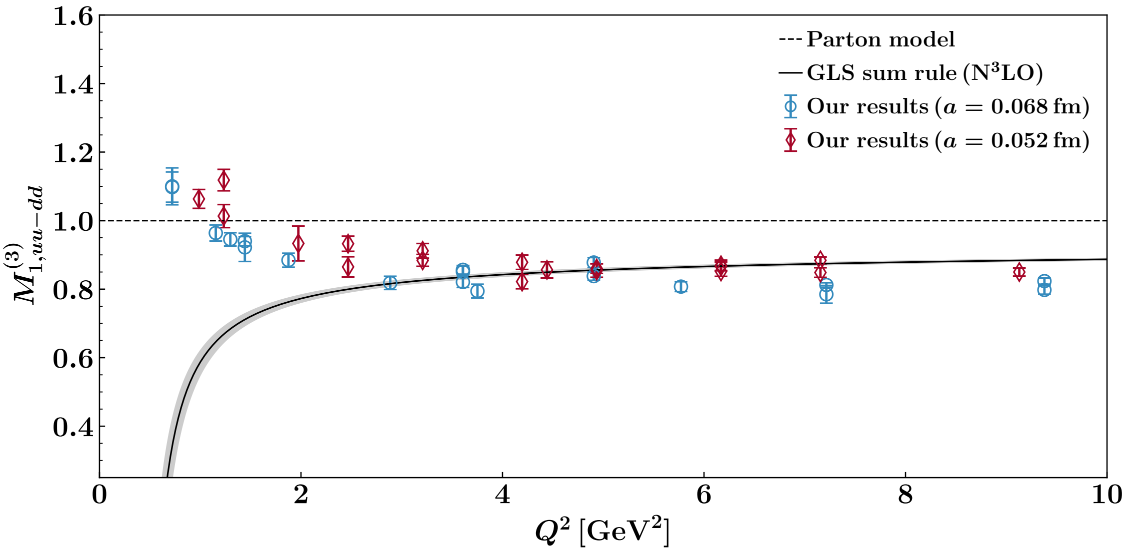

Figure 4: The lowest isovector $uu - dd$ moment of the F_3 structure function as a function of Q^2. Our (corrected) lattice results are compared to the perturbative part of the GLS sum rule analogue for the $F_3^{\gamma Z}$ (Eq. (17) without the higher-twist term).

to the GLS sum rule analogue for the $F_3^{\gamma Z}$,

$$I^{\gamma Z}_{GLS}(Q^2) = (N_u - N_d)\left[1 - \sum_{i=1}^{4} C_i\, a_s^i(Q^2)\right] + \frac{\Delta_q^{\mathrm{HT}}}{Q^2} + \cdots, \tag{17}$$

where $N_u = 2$, and $N_d = 1$, the C_i are known coefficients, $a_s(Q^2) \equiv \alpha_s(Q^2)/\pi$, and Δ^{HT} denote the coefficient of the leading higher-twist term with ellipses denoting the neglected higher-order power corrections. The solid band shown in Fig. 4 is the perturbative part of Eq. (17), i.e. the higher-twist correction term is omitted. We see that our results are in agreement with the perturbative curve in the perturbative region, $Q^2 \gtrsim 4$ GeV^2, while there appears a clear discrepancy towards lower Q^2 values, highlighting non-perturbative effects.

Our preliminary results here provide an intermediate step towards studying higher-twist effects, determining α_s from an hadronic observable, and estimating the electroweak box diagram contributions relevant for V_{ud} or the weak mixing angle.

5. Summary and outlook

In this contribution we have provided an update on our preliminary calculations of the parity-violating Compton amplitude using an extension of the Feynman-Hellmann approach. Our calculations have been performed on QCDSF collaboration's $2+1$ flavour, $48^3 \times 96$ gauge ensembles with $\beta = 5.65$ and $\beta = 5.95$, corresponding to lattice spacings $a = 0.068$ fm and $a = 0.052$ fm, with the light quark masses tuned to approximately the physical flavour-singlet mass yielding $m_\pi \approx 420$ MeV. We have calculated the lowest odd Mellin moment of $F_3^{\gamma Z}$ for photon momenta in the range $0.5 \lesssim Q^2 \lesssim 10$ GeV^2. Our results reach a good statistical precision and reveal the effects of lattice artefacts. We have derived a correction factor to address one of the discretisation artefacts and applied it to our moments. A comparison of our lattice moments to the Gross–Llewellyn Smith sum rule analogue for $F_3^{\gamma Z}$ shows agreement in the perturbative regime while it reveals a clear discrepancy between our results and the perturbative sum rule starting around $Q^2 \lesssim 4$ GeV^2, indicating higher-twist effects. Our results pave the way towards providing valuable input for estimating the electroweak box-diagram contributions to the superallowed nuclear and neutron beta decays and testing the Gross–Llewellyn Smith sum rule, along with determining α_s and studying higher-twist effects.

Acknowledgments

The numerical configuration generation (using the BQCD lattice QCD program [30])) and data analysis (using the Chroma software library [31]) was carried out on the DiRAC Blue Gene Q and Extreme Scaling (EPCC, Edinburgh, UK) and Data Intensive (Cambridge, UK) services, the GCS supercomputers JUQUEEN and JUWELS (NIC, Jülich, Germany) and resources provided by HLRN (The North-German Supercomputer Alliance), the NCI National Facility in Canberra, Australia (supported by the Australian Commonwealth Government) and the Phoenix HPC service (University of Adelaide). RH is supported by STFC through grant ST/X000494/1. PELR is supported in part by the STFC under contract ST/G00062X/1. KUC, RDY and JMZ are supported by the Australian Research Council grant Nos. DP220103098 and DP240102839. For the purpose of open access, the authors have applied a Creative Commons Attribution (CC BY) licence to any Author Accepted Manuscript version arising from this submission.

References

[1] J.C. Hardy and I.S. Towner, *Superallowed* $0^+ \to 0^+$ *nuclear* β *decays: 2014 critical survey, with precise results for* V_{ud} *and CKM unitarity*, *Phys. Rev. C* **91** (2015) 025501 [1411.5987].

[2] K.S. Kumar, S. Mantry, W.J. Marciano and P.A. Souder, *Low Energy Measurements of the Weak Mixing Angle*, *Ann. Rev. Nucl. Part. Sci.* **63** (2013) 237 [1302.6263].

[3] A.S. Kronfeld, D.G. Richards, W. Detmold, R. Gupta, H.-W. Lin, K.-F. Liu, A. S. Meyer, R. Sufian and S. Syritsyn, *Lattice QCD and Neutrino-Nucleus Scattering*, *Eur. Phys. J. A* **55** (2019) 196 [1904.09931].

[4] R. Acciarri et al., *Long-Baseline Neutrino Facility (LBNF) and Deep Underground Neutrino Experiment (DUNE): Conceptual Design Report, Volume 2: The Physics Program for DUNE at LBNF*, 1512.06148.

[5] S. Forte, *Polarized structure functions with neutrino beams*, in *16th International Spin Physics Symposium (SPIN 2004)*, pp. 154–162, 1, 2005, [hep-ph/0501020].

[6] R.D. Ball, L. Del Debbio, S. Forte, A. Guffanti, J.I. Latorre, A. Piccione, J. Rojo and M. Ubiali, *Precision determination of electroweak parameters and the strange content of the proton from neutrino deep-inelastic scattering*, *Nucl. Phys. B* **823** (2009) 195 [0906.1958].

[7] A.J. Chambers, R. Horsley, Y. Nakamura, H. Perlt, P.E.L. Rakow, G. Schierholz, A. Schiller, K. Somfleth, R. D. Young and J. M. Zanotti, *Nucleon structure functions from operator product expansion on the lattice*, *Phys. Rev. Lett.* **118** (2017) 242001 [1703.01153].

[8] K.U. Can, A. Hannaford-Gunn, R. Horsley, Y. Nakamura, H. Perlt, P.E.L. Rakow, G. Schierholz, K. Somfleth, H. Stüben, R. D. Young and J. M. Zanotti, *Lattice QCD evaluation of the Compton amplitude employing the Feynman-Hellmann theorem*, *Phys. Rev. D* **102** (2020) 114505 [2007.01523].

[9] M. Batelaan, K.U. Can, A. Hannaford-Gunn, R. Horsley, Y. Nakamura, H. Perlt, P. E. L. Rakow, G. Schierholz, H. Stüben, R. D. Young and J. M. Zanotti, *Moments and power corrections of longitudinal and transverse proton structure functions from lattice QCD*, *Phys. Rev. D* **107** (2023) 054503 [2209.04141].

[10] K.U. Can, *The Compton amplitude and nucleon structure functions*, *PoS* **LATTICE2022** (2023) 237 [2212.09197].

[11] K.U. Can, R. Horsley, Y. Nakamura, P.E.L. Rakow, G. Schierholz, H. Stuben, R. D. Young and J. M. Zanotti, *The parity-odd structure function of nucleon from the Compton amplitude*, *PoS* **LATTICE2023** (2024) 311 [2402.00255].

[12] P.-X. Ma, X. Feng, M. Gorchtein, L.-C. Jin, K.-F. Liu, C.-Y. Seng, B.-G. Wang and Z.-L. Zhang, *Lattice QCD Calculation of Electroweak Box Contributions to Superallowed Nuclear and Neutron Beta Decays*, *Phys. Rev. Lett.* **132** (2024) 191901 [2308.16755].

[13] A. Retey and J.A.M. Vermaseren, *Some higher moments of deep inelastic structure functions at next-to-next-to-leading order of perturbative QCD*, *Nucl. Phys. B* **604** (2001) 281 [hep-ph/0007294].

[14] S.A. Larin and J.A.M. Vermaseren, *The α_s^3 corrections to the Bjorken sum rule for polarized electroproduction and to the Gross-Llewellyn Smith sum rule*, *Phys. Lett. B* **259** (1991) 345.

[15] L. Hayen, *Standard model $O(\alpha)$ renormalization of g_A and its impact on new physics searches*, *Phys. Rev. D* **103** (2021) 113001 [2010.07262].

[16] V.M. Braun and A.V. Kolesnichenko, *Power corrections to Bjorken and Gross-Llewellyn Smith sum rules in QCD*, *Nucl. Phys. B* **283** (1987) 723.

[17] G.G. Ross and R.G. Roberts, *Improved QCD sum rule estimates of the higher twist contributions to polarized and unpolarized nucleon structure functions*, *Phys. Lett. B* **322** (1994) 425 [hep-ph/9312237].

[18] M. Dasgupta and B.R. Webber, *Power corrections and renormalons in deep inelastic structure functions*, *Phys. Lett. B* **382** (1996) 273 [hep-ph/9604388].

[19] X. Ji, *The nucleon structure functions from deep-inelastic scattering with electroweak currents*, *Nucl. Phys. B* **402** (1993) 217 .

PoS(LATTICE2024)326

[20] A.W. Thomas and W. Weise, *The Structure of the Nucleon*, Wiley, Germany (2001), 10.1002/352760314X.

[21] A. Hannaford-Gunn, K.U. Can, R. Horsley, Y. Nakamura, H. Perlt, P. E. L. Rakow, H. Stüben, G. Schierholz, R. D. Young and J. M. Zanotti, *Generalized parton distributions from the off-forward Compton amplitude in lattice QCD*, *Phys. Rev. D* **105** (2022) 014502 [2110.11532].

[22] M. Constantinou, R. Horsley, H. Panagopoulos, H. Perlt, P.E.L. Rakow, G. Schierholz, A. Schiller and J. M. Zanotti, *Renormalization of local quark-bilinear operators for N_f=3 flavors of stout link nonperturbative clover fermions*, *Phys. Rev. D* **91** (2015) 014502 [1408.6047].

[23] A. Agadjanov, U.-G. Meißner and A. Rusetsky, *Nucleon in a periodic magnetic field*, *Phys. Rev. D* **95** (2017) 031502 [1610.05545].

[24] C.-Y. Seng and U.-G. Meißner, *Toward a First-Principles Calculation of Electroweak Box Diagrams*, *Phys. Rev. Lett.* **122** (2019) 211802 [1903.07969].

[25] W. Bietenholz., V. Bornyakov, N. Cundy, M. Göckeler, R. Horsley, A.D. Kennedy, W. G. Lockhart, Y. Nakamura, H. Perlt, D. Pleiter, P. E. L. Rakow, A. Schäfer, G. Schierholz, A. Schiller, H. Stüben and J. M. Zanotti, *Tuning the strange quark mass in lattice simulations*, *Phys. Lett.* **B690** (2010) 436 [1003.1114].

[26] W. Bietenholz, V. Bornyakov, M. Göckeler, R. Horsley, W.G. Lockhart, Y. Nakamura, H. Perlt, D. Pleiter, P. E. L. Rakow, G. Schierholz, A. Schiller, T. Streuer, H. Stüben, F. Winter and J. M. Zanotti, *Flavour blindness and patterns of flavour symmetry breaking in lattice simulations of up, down and strange quarks*, *Phys. Rev. D* **84** (2011) 054509 [1102.5300].

[27] S. R. Beane, W. Detmold, R. Horsley, M. Illa, M. Jafry, D. J. Murphy, Y. Nakamura, H. Perlt, P. E. L. Rakow, G. Schierholz, P. E. Shanahan, H. Stüben, M. L. Wagman, F. Winter, R. D. Young and J. M. Zanotti, *Charged multihadron systems in lattice QCD+QED*, *Phys. Rev. D* **103** (2021) 054504 [2003.12130].

[28] M. Göckeler, R. Horsley, H. Perlt, P.E.L. Rakow, G. Schierholz and A. Schiller, *Operator product expansion on the lattice: Analytic Wilson coefficients*, *PoS* **LAT2006** (2006) 119 [hep-lat/0610064].

[29] K.U. Can, A. Hannaford-Gunn, R. Horsley, P.E.L. Rakow, T. Schar, G. Schierholz, H. Stüben, R. D. Young and J. M. Zanotti, *A lattice QCD calculation of the Compton amplitude subtraction function*, 2501.08619.

[30] T.R. Haar, Y. Nakamura and H. Stuben, *An update on the BQCD Hybrid Monte Carlo program*, *EPJ Web Conf.* **175** (2018) 14011 [1711.03836].

[31] R.G. Edwards (SciDAC and LHPC Collaboration) and B. Joó (UKQCD Collaboration), *The Chroma software system for lattice QCD*, *Nucl. Phys. Proc. Suppl.* **140** (2005) 832 [hep-lat/0409003].

PoS(LATTICE2024)326